

## Effects of Mass Variation in the Collinear Perturbed Moulton-Copenhagen Configuration

Abdullah A. Ansari<sup>1,2,\*</sup>, Brijendra Yadav<sup>3</sup>

<sup>1</sup>*Department of Mathematics, Shivaji College, University of Delhi, New Delhi, India*

<sup>2</sup>*International Center for Advanced Interdisciplinary Research (ICAIR), Sangam Vihar, New Delhi, India*

<sup>3</sup>*Department of Mathematics, Acharya Narendra Dev College, University of Delhi, New Delhi, India*

\*Corresponding author: [icairndin@gmail.com](mailto:icairndin@gmail.com)

**Abstract.** The main idea of this paper is to investigate the motion properties of the smallest body under the gravitational forces of the three collinear spherical primaries. Here we place the three primaries on the same line where the masses of two primary bodies are taken equal and third primary body is having the solar radiation effect. The effects of Coriolis and centrifugal forces on the system is considered. Therefore this system is recognized as collinear perturbed Moulton-Copenhagen configuration. After determining the equations of motion and quasi-Jacobi integral, we numerically illustrate the locations of equilibrium points (in-plane and out-of-plane), regions of motion, Poincaré surfaces of section, basins of attraction and periodic orbits. And then the examination of stability for the equilibrium points lie either in-plane or out-of-plane are examined.

### 1. Introduction

One of the extensions of the restricted three-body problem is the restricted four-body problem in the fields of Mathematics and theoretical Physics. Where two types of configurations are found in the literature. First when the three-primaries are placed at the vertices of a triangle and the second when the three-primaries are placed at the same horizontal line. Till now many researchers have studied about the first type of configuration with various types of perturbations while the second type of configuration is studied by very few researchers. But it is also an interesting configuration for study.

Received: Jul. 11, 2022.

2010 *Mathematics Subject Classification.* 70F05, 70F15.

*Key words and phrases.* perturbed Moulton-Copenhagen configuration; variable mass; Jeans law; out-of-plane equilibrium points.

We are also interested to study this less studied configuration with variable mass, solar radiation pressure and perturbations in Coriolis as well as centrifugal forces.

We would like to elaborate our literature review about the above said configuration. [1] studied the four-body problem with spherical primaries and investigated the existence and uniqueness of the equilibrium points. [2] performed the relative equilibrium solutions in the restricted four-body problem and also presented the survey of solutions for arbitrary masses. [3] studied the restricted four-body problem. [4] studied the number of equivalence classes in the restricted four body problem. [5] extended the model considered by Arenstorff and studied the collinear relative equilibria of the planar N-body problem. [6] investigated the restricted 3-body problem by supposing both the primaries as solar radiation effects. A complete solution of the problems of existence and linear stability of the equilibrium points are performed for various values of radiation pressure. They found one of the Lagrangian points is stable when both the primaries are having radiation pressure. Four out-of-plane equilibrium points exists when the radiation pressure of the smaller body is very high. When both the primaries are luminous then  $L_{8,9}$  are linearly unstable while  $L_{6,7}$  are stable for an interval of radiation pressure. [7] investigated the restricted three-body problem by supposing the solar radiation pressure. And found the stability of the orbits.

[8] investigated the symmetrical central configuration in three cases and discussed their bifurcations as well as spectral stability. His results are applicable in the rational parameterizations and computer algebra. [9] investigated the asymptotic solutions of the restricted planar problem of four bodies out of which two equal primaries are placed at the same line with equal distance. They got atmost six equilibrium points. They also illustrated numerically the Poincaré cuts, homo-and hetero-clinic, symmetric and non-symmetric asymptotic orbits by using forward and backward integration. They also perform the characteristic curves for a fixed value of the mass parameter and the stability of these families of curves. [10] examined the stability of the periodic orbits in the frame of four-body problem where three-primary bodies are placed in the same straight line. And these bodies are moving around their center of mass. [11] studied the restricted four-body problem where three spherical primaries are placed at the vertices of a triangle. After formulation of the equations of motion, they have found eleven equilibrium points. [12] illustrated the restricted four bodies problem. They also analyzed numerically allowed regions and zero velocity surfaces. [13] investigated the motion properties of the fourth body under the gravitational forces and solar radiation pressures of the three primaries which are placed at the vertices of an equilateral triangle. They observed that the perturbation parameters used are influenced the locations of the equilibrium points and their stability. [14] studied the restricted four-body problem with radiation pressure and they performed the complete analysis of the position of equilibria and their stability in the space. [15] investigated three-dimensional case of the restricted four-body problem with equal radiation pressures. They present the complete study of position and

stability of equilibrium points. [16] investigated the planar restricted four-body problem in the Moulton-Copenhagen configuration. They performed the evolution of families of symmetric periodic orbits as the mass parameter  $\mu$  evolves. They also analysed the evolution of spiral points which represents the heteroclinic orbits connecting to equilibrium points. [17] performed the dynamics of the circular restricted 4-body problem with three primaries at the collinear configuration. And they examined the linear stability of the equilibrium points. They also proved the existence of periodic orbits by applying the Lyapunov theorem.

The effect of variation of mass is studied by many researchers: [18] determined the equations of motion of the variable mass infinitesimal body in the restricted three-body problem by using the Lagrangian approach. To conserve the time in space, they have used the Meshcherskii transformation. [19] illustrated the mass variation effects in the restricted four-body problem by supposing that the primaries are moving in elliptical orbits around their common center of mass. [20] performed the dynamical properties of the infinitesimal body in the restricted six-body problem under the consideration that the infinitesimal body varies its mass according to the Jeans law. After an adequate formulation, they have illustrated the equilibrium points, regions of motion and basins of attraction for this model. [21] extended the idea of [18] and found the all the equilibrium points are unstable for this model. [22–24] also studied the variation effects of the mass of the infinitesimal body in the restricted problems.

This manuscript is arranged in various sections as: Overview of the literature is presented in section 1. The equations of motion and quasi-Jacob integral are performed in section 2 while section 3 presents the locations of equilibrium points. Sections 4 illustrate the regions of motion and section 5 explained the Poincaré surfaces of section. Section 6 and 7 illustrate the basins of attraction and periodic orbits respectively. Finally examination of the stability for the equilibrium points are done in section 8, and drawn the conclusion in section 9.

## 2. Equations of motion

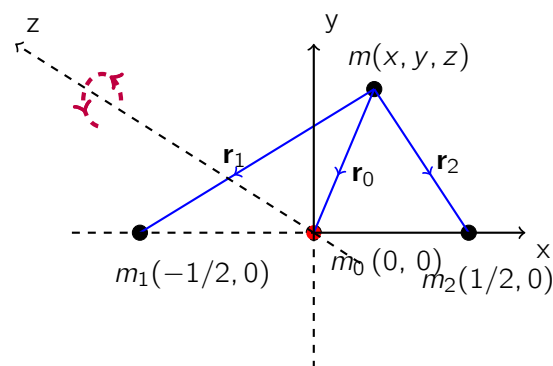


Figure 1. Collinear perturbed Moulton-Copenhagen configuration

Out of four bodies, the collinear placed three bodies are known as primaries of masses  $m_0$ ,  $m_1$ , and  $m_2$  respectively. The fourth smallest body is moving in space under the gravitational forces of the

three primaries while the smallest body is not affecting them (figure-1). The primary of mass  $m_0$  is having the effect of solar radiation pressure with radiation parameter  $\beta_0$ . We also assume that the Coriolis and centrifugal forces are affecting to the system with parameters  $\alpha_1$  and  $\alpha_2$ . Considering the synodic axis and fixing the units of  $G m_1$ ,  $G m_2$  and the distance between two primaries  $m_1 m_2$ , separately taken as unity and also  $G m_0 = \mu$ , we get the value of mean motion  $\omega$  as  $\sqrt{2(1 + 4\mu)}$ .

Adopting the method used by [25] and [16], the equations of motion of the smallest body of variable mass can be written as:

$$\begin{aligned} \frac{\dot{m}}{m}(\dot{x} - \omega \alpha_1 y) + \ddot{x} - 2\omega \alpha_1 \dot{y} &= \frac{\partial \Omega}{\partial x}, \\ \frac{\dot{m}}{m}(\dot{y} + \omega \alpha_1 x) + \ddot{y} + 2\omega \alpha_1 \dot{x} &= \frac{\partial \Omega}{\partial y}, \\ \frac{\dot{m}}{m} \dot{z} + \ddot{z} &= \frac{\partial \Omega}{\partial z}, \end{aligned} \quad (2.1)$$

where,

$$\begin{aligned} \Omega &= \frac{1}{2} \omega^2 \alpha_2 (x^2 + y^2) + \frac{\mu \beta_0}{r_0} + \frac{1}{r_1} + \frac{1}{r_2}, \\ r_0^2 &= x^2 + y^2 + z^2, \\ r_1^2 &= (x + 1/2)^2 + y^2 + z^2, \\ r_2^2 &= (x - 1/2)^2 + y^2 + z^2. \end{aligned} \quad (2.2)$$

We have considered the mass variation of the smallest body therefore we can not investigate the motion properties directly and hence we will follow the Jean's law [26] and Meshcherskii space-time transformations [27] which are as follow:

$$m = m_{init} e^{-\epsilon_1 t}, \quad (x, y, z) = \frac{1}{\sqrt{\epsilon_2}} (\xi, \eta, \zeta), \quad (2.3)$$

where  $\epsilon_1$  is variation constant and  $\epsilon_2 = \frac{m}{m_{init}}$ , where  $m_{init}$  is the initial mass of the smallest body. Utilizing Eqs. (2.1) and (2.3), we obtain

$$\begin{aligned} \ddot{\xi} - 2\omega \alpha_1 \dot{\eta} &= \frac{\partial V}{\partial \xi}, \\ \ddot{\eta} + 2\omega \alpha_1 \dot{\xi} &= \frac{\partial V}{\partial \eta}, \\ \ddot{\zeta} &= \frac{\partial V}{\partial \zeta}, \end{aligned} \quad (2.4)$$

where,

$$V = \frac{\omega^2 \alpha_2}{2} (\xi^2 + \eta^2) + \frac{\epsilon_1^2}{8} (\xi^2 + \eta^2 + \zeta^2) + \epsilon_2^{3/2} \left\{ \frac{\mu \beta_0}{\rho_0} + \frac{1}{\rho_1} + \frac{1}{\rho_2} \right\},$$

$$\begin{aligned} \rho_0^2 &= \xi^2 + \eta^2 + \zeta^2, \\ \rho_1^2 &= (\xi + \sqrt{\epsilon_2}/2)^2 + \eta^2 + \zeta^2, \\ \rho_2^2 &= (\xi - \sqrt{\epsilon_2}/2)^2 + \eta^2 + \zeta^2. \end{aligned} \quad (2.5)$$

The Eq. (2.4) reveals the Quasi-Jacobi integral as

$$(\dot{\xi}^2 + \dot{\eta}^2 + \dot{\zeta}^2) = 2V - E - 2 \int_{t_0}^t \left( \frac{\partial V}{\partial t} \right) dt, \quad (2.6)$$

where E is the quasi-Jacobi energy constant. If we suppose  $\epsilon_1 = 0$  and  $\epsilon_2 = 1$ , then the above variable mass system will reduce to the constant mass system.

### 3. Equilibrium points

Taking zero to all derivatives w.r.t. time in Eq. (2.4), we get

$$\frac{\partial V}{\partial \xi} = 0, \quad (3.1a)$$

$$\frac{\partial V}{\partial \eta} = 0, \quad (3.1b)$$

$$\frac{\partial V}{\partial \zeta} = 0. \quad (3.1c)$$

After numerically solving Eqs. (3.1a) and (3.1b) by taking  $\zeta = 0$ , we get the equilibrium points in in-plane motion while solving Eqs. (3.1a) and (3.1c) by taking  $\eta = 0$ , we get the out-of-plane equilibrium points. We will discuss about these equilibrium points in two sub-sections in-plane equilibrium points and out-of-plane equilibrium points. (In this calculations, we have used  $\epsilon_1 = 0.2$ ,  $\epsilon_2 = 0.4$ ,  $\alpha_1 = \alpha_2 = 1.2$ ,  $\mu = 0.25$ ,  $\beta_0 = 0.95$ .)

**3.1. In-plane equilibrium points.** After numerically solving Eqs. (3.1a) and (3.1b) by taking  $\zeta = 0$ , we get six in-plane equilibrium points out of which four are collinear equilibrium points  $L_{1,2,3,4}$  and two are non-collinear equilibrium points  $L_{5,6}$ . These equilibrium points are presented in figure (2). We observed from this figure that out of four collinear equilibrium points, two  $L_{1,2}$  and  $L_{3,4}$  are symmetrical about  $\eta$ -axis respectively as well as  $L_{5,6}$  are symmetrical about  $\xi$ -axis. We have plotted these for various values of variation parameters ( $\epsilon_1 = 0$  &  $\epsilon_2 = 1$  (red),  $\epsilon_1 = 0.2$  &  $\epsilon_2 = 0.8$  (blue), 0.4 (purple), and given in the sub-figure (2(a)). We observed from here that as increase the value of the parameter  $\epsilon_2$ , locations of the equilibrium points are moving away. The sub-figure (2(b)) shows the locations of the equilibrium points for the variation of the centrifugal force parameter  $\alpha_2 = 1.2$  (purple), 1.6 (blue) and 2 (red). This sub-figure reveals that as increase the value of the parameter

$\alpha_2$ , the locations of equilibrium points  $L_{2,3}$  are unchanged while the locations of equilibrium points  $L_{1,4,5,6}$  are moving towards the origin. Finally, it is also observed that when the primaries are placed at the vertices of an equilateral triangle, there are eleven equilibrium points exist [11] while when the three primaries are placed on the same straight line then we got six equilibrium points.

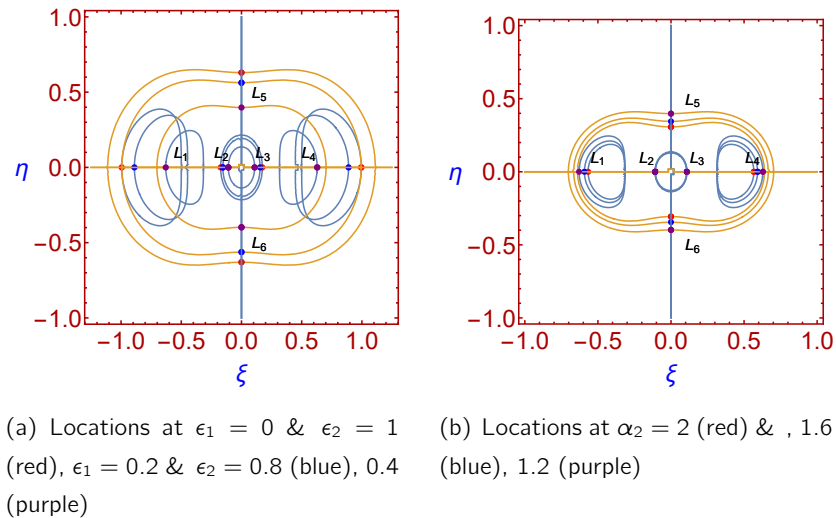


Figure 2. Locations of in-plane equilibrium points.

3.2. **Out-of-plane equilibrium points.** And when we numerically solve Eqs. (3.1a) and (3.1c) by taking  $\eta = 0$ , we get the out-of-plane equilibrium points and we noticed here that when we plotted the locations of equilibrium points for the constant mass, then there is no out-of-plane equilibrium point (sub-figure (3(a))) while when we consider the variable mass case then we got two out-of-plane equilibrium points ( $L_{7,8}$ ) along  $\zeta$ -axis (sub-figure (3(b))). The equilibrium points ( $L_{7,8}$ ) are symmetrical about  $\xi$ -axis. These two equilibrium points are additional evaluation in this research.

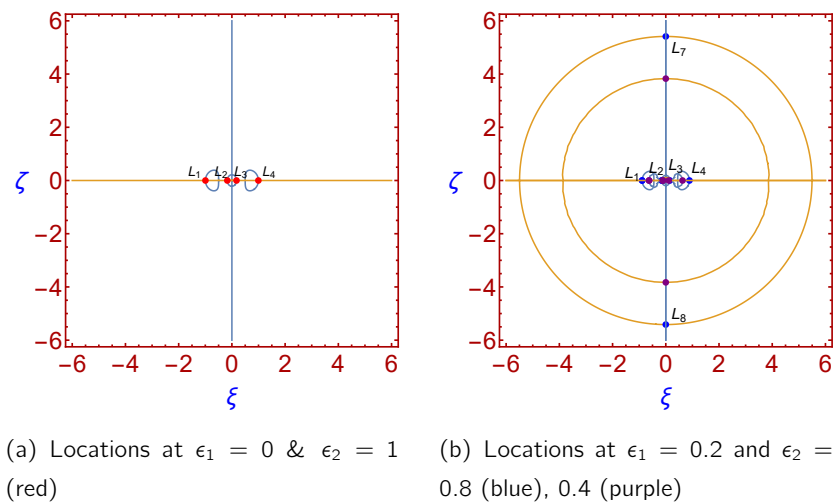


Figure 3. Locations of out-of-plane equilibrium points.

### 4. Regions of motion

Utilising the method given by [28], we have performed the regions of motion of the smallest body for various values of the variation parameters used and given in figures (3) (at  $\epsilon_1 = 0, \epsilon_2 = 1$ ) and (4) (at  $\epsilon_1 = 0, \epsilon_2 = 0.4$ ). To illustrate the regions of motion, we have to evaluate first the value of energy constant (E) corresponding to equilibrium points and then with the help of this value, we have performed the allowed regions of motion. These regions are shown in the figures as white parts while colored parts are prohibited regions. In both the figures, sub-figures (a), (b) and (c) are representing the regions corresponding to the equilibrium points  $L_{1,4}, L_{2,3}$  and  $L_{5,6}$  respectively. The sub-figure (a) reveals that smallest body can move every where except near the equilibrium points  $L_{5,6}$  and the equilibrium points  $L_{1,4}$  act as gateway for the regions near the equilibrium points  $L_{2,3}$ . The sub-figure (b) reveals that the smallest body can move every where except near the equilibrium points  $L_{1,4,5,6}$  and the parking points  $L_{2,3}$  act as gateway for the regions around the equilibrium points  $L_{2,3}$ . The sub-figure (c) reveals that the smallest body can move every where and there is no prohibited regions. The main difference in both the figures that as reduces the value of variation parameter  $\epsilon_2$ , the regions are shrinking.

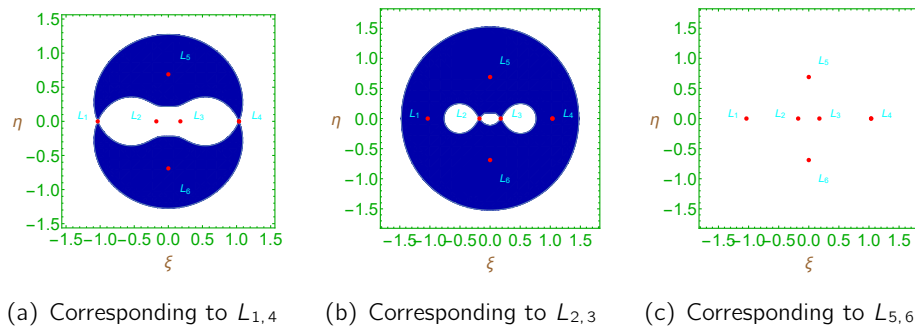


Figure 4. Regions of motion at  $\epsilon_1 = 0$  &  $\epsilon_2 = 1$  in  $\xi - \eta$ -plane.

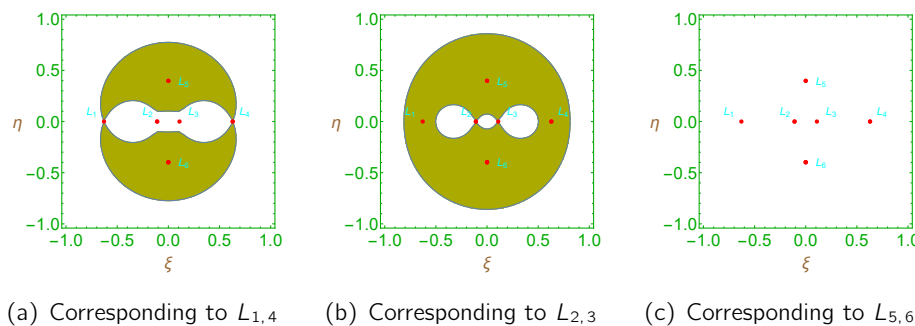
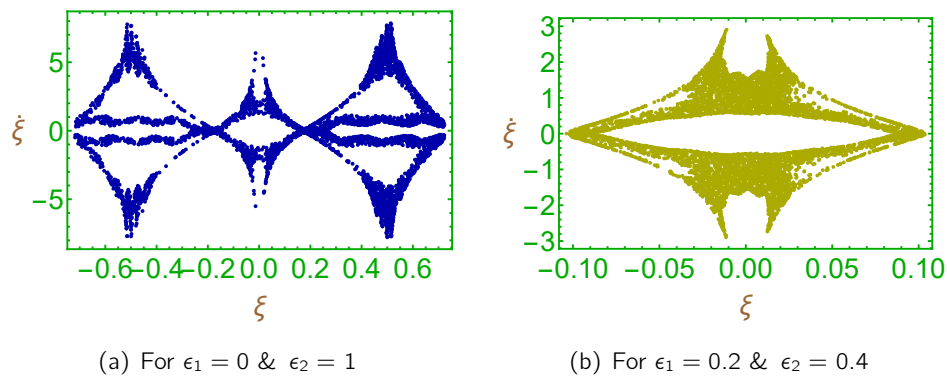
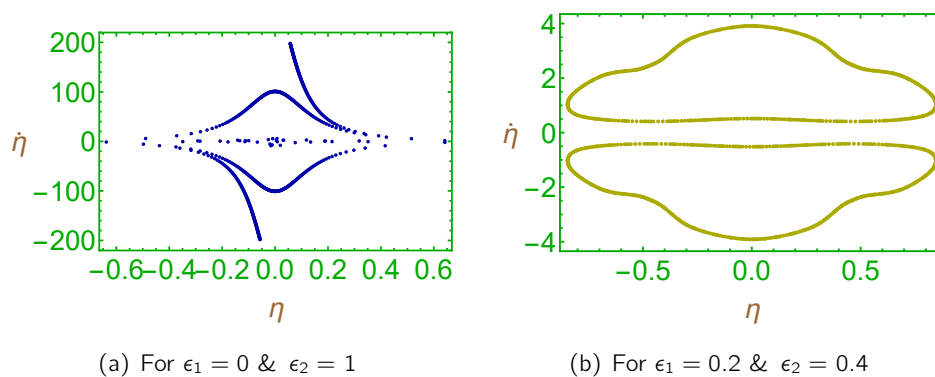


Figure 5. Regions of motion at  $\epsilon_1 = 0.2$  &  $\epsilon_2 = 0.4$  in  $\xi - \eta$ -plane.

## 5. Poincaré surfaces of section

This section performed the Poincaré surfaces of section with the help of Eqs. (2.4) and (2.6). For this, we have to rewrite the system of equations into phase space and then draw until when the orbit intersects the plane  $\dot{\eta} \geq 0$ . Finally, we get the surfaces of section in  $\xi - \dot{\xi}$ -plane by using well known Mathematica software for various values of the variation parameters and given in figure (6). Sub-figure (6(a)) perform the Poincaré surfaces of section with three shapes for the value of  $\epsilon_1 = 0$  and  $\epsilon_2 = 1$  (blue). We observed from here that these surfaces are symmetrical about both axes and also as we move away from the origin on the middle shape along  $\dot{\xi}$ -axis, there are some chaos. Some chaos are found on the other two shapes also. As we have supposed the effects of the variation parameters ( $\epsilon_1 = 0.2$  and  $\epsilon_2 = 0.4$  (dark yellow)), three shapes are reduced to a single shape, which is also symmetrical about both axes. We observed from here that there are some partial chaos at some places. For the same two cases (constant mass case (sub-figure-(7(a))) (blue) and variable mass case (sub-figure-(7(b)))(dark yellow)), we have plotted the Poincaré surfaces of section in  $\eta - \dot{\eta}$ -plane and observed that in the constant mass case there are chaos along  $\eta$ -axis only while there is no chaos in the variable mass case.

Figure 6. Poincaré surfaces of section in  $\xi - \dot{\xi}$ -plane.Figure 7. Poincaré surfaces of section in  $\eta - \dot{\eta}$ -plane.

### 6. Basins of attraction

Basins of attracting domain is also one of the most important dynamical behaviour of the smallest body. In this section, we have illustrated the basins of attraction of the smallest body by using very fast, simple and accurate method known as Newton-Raphson method. This attracting domain is the composition of all initial conditions that converge to specific equilibrium points. Here we have plotted the basins of attracting domain in two  $\xi - \eta$  and  $\xi - \zeta$  planes. The formula used for this problem is as follows:

$$\xi_{n+1} = \xi_n - \frac{V_\xi V_{\eta\eta} - V_\eta V_{\xi\eta}}{V_{\xi\xi} V_{\eta\eta} - V_{\xi\eta} V_{\eta\xi}},$$

$$\eta_{n+1} = \eta_n - \frac{V_\eta V_{\xi\xi} - V_\xi V_{\xi\eta}}{V_{\xi\xi} V_{\eta\eta} - V_{\xi\eta} V_{\eta\xi}},$$
(6.1)

where  $\xi_n$  and  $\beta_n$  are the values of  $n^{th}$  step for  $\xi$  and  $\eta$  in the Newton-Raphson iterative process.  $(\xi, \eta)$  will be a member of the attracting domain if the initial point converges rapidly to one of the equilibrium points. This process stops when it will converges to an attractor. The classification of equilibrium points on the plane will be differentiated by the color code.

The figure (8) shows the basins of attracting domain for two values of variation parameters  $\epsilon_2$  ( $= 1$  (8(a)) and  $0.4$  (8(b))) in the  $\xi - \eta$ -plane. The sub-figures (8(a)) and (8(b)) show that the attracting points  $L_{1,2,3,4}$  represent the cyan and yellow color regions respectively. In the same sequence of the figures  $L_{5,6}$  represent (purple, yellow) and (green, orange) color regions respectively. The basins of attracting domain for all these points extend to infinity.

Similar way we can say that figure (9) corresponds to the basins of attracting domain in the  $\xi - \zeta$ -plane. We observed from here that the equilibrium points  $L_{7,8}$  represent the red color regions which are also extending to infinity. In this way, we got the final version of the basins of attracting domain.

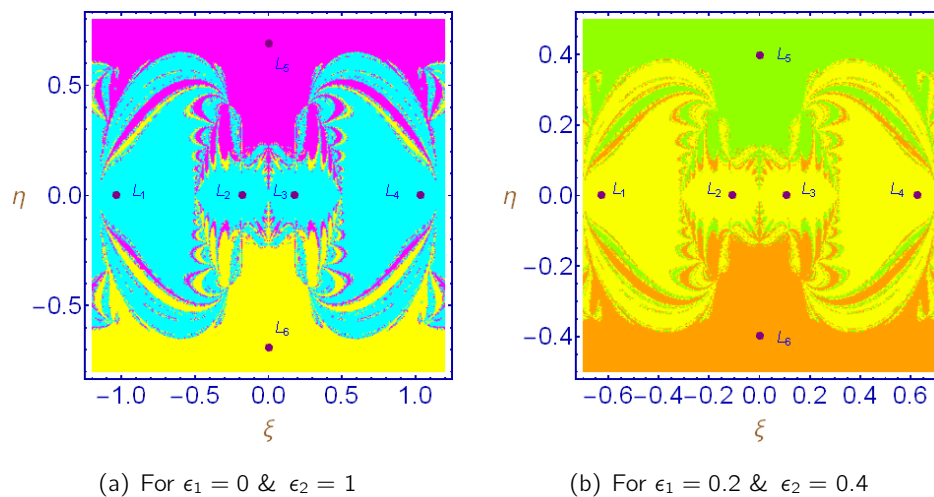
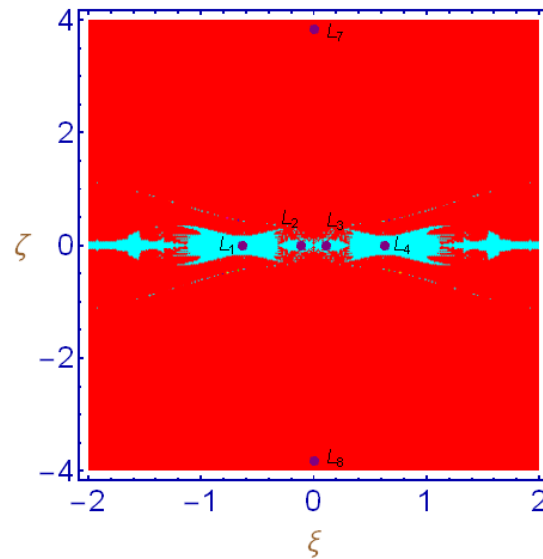
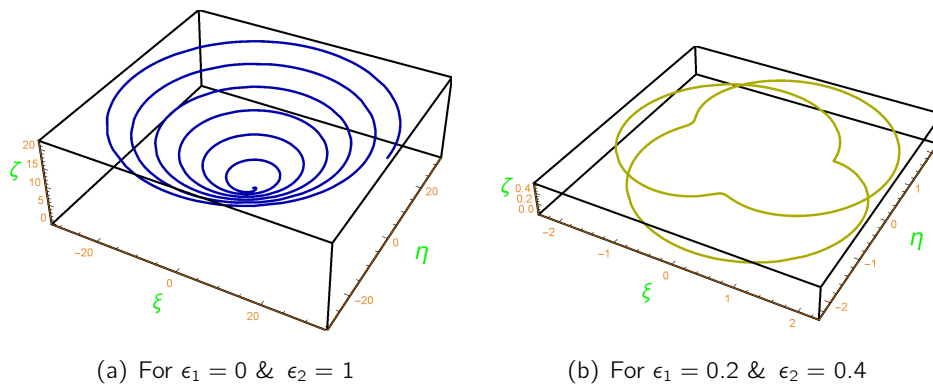


Figure 8. Basins of attracting domain in  $\xi - \eta$ -plane.

(a) For  $\epsilon_1 = 0.2$  &  $\epsilon_2 = 0.4$ Figure 9. Basins of attracting domain in  $\xi - \zeta$ -plane.

### 7. Periodic orbits

We also have plotted the periodic orbits for the motion of smallest body for the two values of variation parameter  $\epsilon_2$  ( $= 1$  (blue) (10(a)) and  $0.4$  (dark yellow) (10(b))). To perform this, we have numerically solved Eq. (2.4) through well known software mathematica and plotted the periodic orbits in 3D. There is no periodic orbits when  $\epsilon_2 = 1$  while we get the periodic orbits when  $\epsilon_2 = 0.4$ . i.e. in the variable mass case we get the periodic orbits with period 8.87 units.

(a) For  $\epsilon_1 = 0$  &  $\epsilon_2 = 1$ (b) For  $\epsilon_1 = 0.2$  &  $\epsilon_2 = 0.4$ Figure 10. Periodic orbits in  $\xi - \eta - \zeta$ -plane.

### 8. Stability states

Utilizing the method adopted by [29], we shall examine numerically the stability states for the equilibrium points. Since  $L_{1,2}$  and  $L_{3,4}$  are symmetrical about  $\eta$ -axis as well as  $L_5$  and  $L_6$  are

symmetrical about  $\xi$ -axis. Therefore examination of the stability of  $L_{1,2,5}$  are sufficient to show the stability of all equilibrium points. And hence we can write the characteristic polynomial of the Eq. (2.4) as:

$$\lambda^6 + D_5 \lambda^5 + D_4 \lambda^4 + D_3 \lambda^3 + D_2 \lambda^2 + D_1 \lambda + D_0 = 0, \quad (8.1)$$

where

$$\begin{aligned} D_5 &= -3\epsilon_1, \\ D_4 &= 4\alpha_1^2\omega^2 - (V_{\xi\xi})^0 - (V_{\eta\eta})^0 - (V_{\zeta\zeta})^0 + \frac{15}{4}\epsilon_1^2, \\ D_3 &= 2\epsilon_1((V_{\xi\xi})^0 + (V_{\eta\eta})^0 + (V_{\zeta\zeta})^0) - \frac{5}{4}\epsilon_1^2 - 4\alpha_1^2\omega^2 \\ D_2 &= \frac{15}{16}\epsilon_1^4 + \frac{3}{2}\epsilon_1^2(4\alpha_1^2\omega^2 - (V_{\xi\xi})^0 - (V_{\eta\eta})^0 - (V_{\zeta\zeta})^0) \\ &\quad - [4\alpha_1^2\omega^2 - (V_{\xi\xi})^0 - (V_{\eta\eta})^0](V_{\zeta\zeta})^0 \\ &\quad + ((V_{\xi\eta})^0)^2 + ((V_{\xi\zeta})^0)^2 + ((V_{\eta\zeta})^0)^2 - (V_{\xi\xi})^0(V_{\eta\eta})^0, \\ D_1 &= -\frac{3}{16}\epsilon_1^5 + \frac{\epsilon_1^3}{2}\{(V_{\xi\xi})^0 + (V_{\eta\eta})^0 + (V_{\zeta\zeta})^0 - 4\alpha_1^2\omega^2\} \\ &\quad + \epsilon_1 [((V_{\xi\eta})^0)^2 + ((V_{\xi\zeta})^0)^2 + ((V_{\eta\zeta})^0)^2 - (V_{\xi\xi})^0(V_{\eta\eta})^0 \\ &\quad + \{4\alpha_1^2\omega^2 - (V_{\xi\xi})^0 - (V_{\eta\eta})^0\}(V_{\zeta\zeta})^0], \\ D_0 &= \frac{1}{64}\epsilon_1^6 + \frac{1}{16}\epsilon_1^4\{4\alpha_1^2\omega^2 - (V_{\xi\xi})^0 - (V_{\eta\eta})^0 - (V_{\zeta\zeta})^0\} \\ &\quad - \frac{1}{4}\epsilon_1^2[\{4\alpha_1^2\omega^2 - (V_{\xi\xi})^0 - (V_{\eta\eta})^0\}(V_{\zeta\zeta})^0 + ((V_{\xi\eta})^0)^2 + ((V_{\xi\zeta})^0)^2 \\ &\quad + ((V_{\eta\zeta})^0)^2 - (V_{\xi\xi})^0(V_{\eta\eta})^0] + ((V_{\xi\zeta})^0)^2(V_{\eta\eta})^0 + (V_{\xi\xi})^0((V_{\eta\zeta})^0)^2 \\ &\quad + ((V_{\xi\eta})^0)^2(V_{\zeta\zeta})^0 - (V_{\xi\xi})^0(V_{\eta\eta})^0(V_{\zeta\zeta})^0 - (V_{\xi\eta})^0(V_{\xi\zeta})^0(V_{\eta\zeta})^0. \end{aligned} \quad (8.2)$$

The superscript zero represents the values of the derivatives of the potential function  $V$  corresponding to the equilibrium point. For the constant mass case, the odd coefficients  $D_5$ ,  $D_3$  and  $D_1$  will be zero. We have numerically solved Eq. (8.1) for the variable mass case corresponding to the equilibrium points and given in tables (1, 2, 3 and 4) from where we confirmed that all the equilibrium points

either in-plane or out-of-plane are unstable because all the roots have either at-least one positive real root or a positive real part of the complex roots.

Table 1. The nature of in-plane equilibrium points at  $\epsilon_1 = 0$ ,  $\epsilon_2 = 1$ ,  $\alpha_2 = 1$  and  $\beta_0 = 1$ .

<i>Equilibrium Point</i>		<i>Roots</i>	<i>Nature</i>
$\xi - Co.$	$\eta - Co.$		
$\pm 1.0356396848$	0.0000000000	$\pm 2.6473050713 i$ $\pm 2.8061479556 i$ $\pm 2.6234882293$	<i>Unstable</i>
$\pm 0.1761807154$	0.0000000000	$\pm 8.8544129960 i$ $\pm 8.9276549619 i$ $\pm 12.2516795838$	<i>Unstable</i>
0.0000000000	$\pm 0.6894807659$	$\pm 1.3003188696 \pm 1.9211530815 i$ $0.0000000000 \pm 2.0000000004 i$	<i>Unstable</i>

Table 2. The nature of in-plane equilibrium points at  $\epsilon_1 = 0.2$ ,  $\epsilon_2 = 0.4$ ,  $\alpha_2 = 1.2$  and  $\beta_0 = 0.95$ .

<i>Equilibrium Point</i>		<i>Roots</i>	<i>Nature</i>
$\xi - Co.$	$\eta - Co.$		
$\pm 0.6288018960$	0.0000000000	$0.0999999999 \pm 3.4738810655 i$ $0.1000000016 \pm 2.9690461144 i$ $\pm 2.6336942928$	<i>Unstable</i>
$\pm 0.1092538595$	0.0000000000	$0.0999999999 \pm 8.8249482704 i$ $0.1000000438 \pm 8.9883987793 i$ $- 11.9524281617$ $12.1524281617$	<i>Unstable</i>
0.0000000000	$\pm 0.3977956241$	$- 0.9888291999 \pm 2.3431920592 i$ $0.1000000000 \pm 2.1908902302 i$ $1.1888291999 \pm 2.3431920592 i$	<i>Unstable</i>

Table 3. The nature of in-plane equilibrium points at  $\epsilon_1 = 0.2, \epsilon_2 = 0.4, \alpha_2 = 1.6$  and  $\beta_0 = 0.95$ .

<i>Equilibrium Point</i>		<i>Roots</i>	<i>Nature</i>
$\xi - Co.$	$\eta - Co.$		
$\pm 0.5923124748$	0.0000000000	$0.0999999999 \pm 4.8786946978 i$ $0.1000000002 \pm 3.5550084695 i$ - 2.7826632083 2.9826632083	<i>Unstable</i>
$\pm 0.1081823998$	0.0000000000	$0.0999999992 \pm 8.8796742957 i$ $0.1000000034 \pm 9.3056717985 i$ - 11.6181117601 11.8181117601	<i>Unstable</i>
0.0000000000	$\pm 0.3447013956$	$0.0999999959 \pm 2.2502672920 i$ $0.0999999996 \pm 4.0824376436 i$ $0.1000000049 \pm 2.5298221281 i$	<i>Unstable</i>

Table 4. The nature of out-of-plane equilibrium points at  $\epsilon_1 = 0.2, \epsilon_2 = 0.4, \alpha_2 = 1.2$  and  $\beta_0 = 0.95$ .

<i>Equilibrium Point</i>		<i>Roots</i>	<i>Nature</i>
$\xi - Co.$	$\zeta - Co.$		
0.0000000000	$\pm 3.8279383927$	$0.1000000000 \pm 1.4202504309 i$ $0.1000000003 \pm 3.3797495688 i$ - 0.0726801523 0.2726801523	<i>Unstable</i>

### 9. Conclusion

The motion properties of the smallest body is investigated under the influence of three spherical primaries placed on the same horizontal line. Out of these bodies, one is placed at the common center (also taken as origin) of the other two primaries bodies which are placed at equal distance from the origin. The third primary body is having the effects of solar radiation pressure and the smallest body is varying its mass according to the Jeans law. We also have taken the perturbation effects of

Coriolis and centrifugal forces. The determined perturbed equations of motion and the quasi-Jacobi integral are shown the effects of the perturbations taken by us. After numerical evaluations from the system of equations of motion, we found eight equilibrium points, out of these equilibrium points, six are in-plane equilibrium points and two are out-of-plane equilibrium points. In the in-plane equilibrium points, four are collinear i.e. lie on the  $\xi$ -axis and two are non-collinear i.e. lie on the  $\eta$ -axis as well as two out-of-plane equilibrium points are lie on the  $\zeta$ -axis. We observed from the figures for the in-plane equilibrium points that as increase the values of the variation parameters ( $\epsilon_1$  and  $\epsilon_2$ ) and the perturbation in centrifugal force, the locations of the equilibrium points are moving away and towards the origin respectively. While the perturbation in Coriolis force is not affecting the location of equilibrium points. We also observed that there is no out-of-plane equilibrium points in the constant mass case while two out-of-plane equilibrium points are exists in the variable mass case. And as increase the values of the variation parameters, the locations of the equilibrium points are moving away from the origin. The allowed and prohibited regions of motion are illustrated corresponding to each equilibrium points. Where the shaded regions shown the prohibited regions and white regions corresponds to the allowed regions. From here we revealed that as increase the value of the variation parameters, the shaded regions shrink. Next in the Poincaré surfaces of section, we observed that surfaces are symmetrical about both the axes except the case of constant mass in the  $\eta$ - $\dot{\eta}$ -plane. We also found the chaos at some places of the surfaces. In the basins of attraction section, it is found that all the eight attracting points are extending to infinity. We also plotted the periodic orbits in three-dimensions for both the cases (Constant mass case and variable mass case) and observed that in the constant mass case orbits move spirally upward which is not periodic while in the variable mass case the orbit is periodic with time period 8.87 units. Finally, we have examined the stability of all equilibrium points (in-plane and out-of-plane) and found that all these equilibrium points are unstable.

**Conflicts of Interest:** The authors declare that there are no conflicts of interest regarding the publication of this paper.

## References

- [1] K.B. Bhatnagar, Periodic orbits of collision in the plane circular problem of four bodies, *Indian J. Pure Appl. Math.* 2 (1970), 583–596.
- [2] C. Simo, Relative equilibrium solutions in the four body problem, *Celest. Mech.* 18 (1978), 165-184. <https://doi.org/10.1007/bf01228714>.
- [3] M. Michalodimitrakis, The circular restricted four-body problem, *Astrophys. Space Sci.* 75 (1981), 289-305. <https://doi.org/10.1007/bf00648643>.
- [4] R.F. Arenstorf, Central configurations of four bodies with one inferior mass, *Celest. Mech.* 28 (1982), 9-15. <https://doi.org/10.1007/bf01230655>.
- [5] J.I. Palmore, Collinear relative equilibria of the planarN-body problem, *Celest. Mech.* 28 (1982), 17-24. <https://doi.org/10.1007/bf01230656>.

- [6] J.F.L. Simmons, A.J.C. McDonald, J.C. Brown, The restricted 3-body problem with radiation pressure, *Celest. Mech.* 35 (1985), 145-187. <https://doi.org/10.1007/bf01227667>.
- [7] C.G. Zagouras, Periodic motion around the triangular equilibrium points of the photogravitational restricted problem of three bodies, *Celest. Mech. Dyn. Astr.* 51 (1991), 331-348. <https://doi.org/10.1007/bf00052926>.
- [8] E.S.G. Leandro, On the central configurations of the planar restricted four-body problem, *J. Differ. Equ.* 226 (2006), 323-351. <https://doi.org/10.1016/j.jde.2005.10.015>.
- [9] K.E. Papadakis, Asymptotic orbits in the restricted four-body problem, *Planet. Space Sci.* 55 (2007), 1368-1379. <https://doi.org/10.1016/j.pss.2007.02.005>.
- [10] T.J. Kalvouridis, M. Arribas, A. Elipe, Parametric evolution of periodic orbits in the restricted four-body problem with radiation pressure, *Planet. Space Sci.* 55 (2007), 475-493. <https://doi.org/10.1016/j.pss.2006.07.005>.
- [11] A.N. Baltagiannis, K.E. Papadakis, Equilibrium points and their stability in the restricted four-body problem, *Int. J. Bifurcation Chaos.* 21 (2011), 2179-2193. <https://doi.org/10.1142/s0218127411029707>.
- [12] J.P. Papadouris, K.E. Papadakis, Equilibrium points in the photogravitational restricted four-body problem, *Astrophys. Space Sci.* 344 (2012), 21-38. <https://doi.org/10.1007/s10509-012-1319-8>.
- [13] J. Singh, A.E. Vincent, Equilibrium points in the restricted four-body problem with radiation pressure, *Few-Body Syst.* 57 (2015), 83-91. <https://doi.org/10.1007/s00601-015-1030-8>.
- [14] M. Arribas, A. Abad, A. Elipe, et al. Equilibria of the symmetric collinear restricted four-body problem with radiation pressure, *Astrophys. Space Sci.* 361 (2016), 84. <https://doi.org/10.1007/s10509-016-2671-x>.
- [15] M. Arribas, A. Abad, A. Elipe, et al. Out-of-plane equilibria in the symmetric collinear restricted four-body problem with radiation pressure, *Astrophys. Space Sci.* 361 (2016), 270. <https://doi.org/10.1007/s10509-016-2858-1>.
- [16] M. Palacios, M. Arribas, A. Abad, A. Elipe, Symmetric periodic orbits in the Moulton-Copenhagen problem, *Celest. Mech. Dyn. Astr.* 131 (2019), 16. <https://doi.org/10.1007/s10569-019-9893-5>.
- [17] J. Llibre, D. Paşca, C. Valls, The circular restricted 4-body problem with three equal primaries in the collinear central configuration of the 3-body problem, *Celest. Mech. Dyn. Astr.* 133 (2021), 53. <https://doi.org/10.1007/s10569-021-10052-6>.
- [18] J. Singh, B. Ishwar, Effect of perturbations on the stability of triangular points. In the restricted problem of three bodies with variable mass, *Celest. Mech.* 35 (1985), 201-207. <https://doi.org/10.1007/bf01227652>.
- [19] A.A. Ansari, S.N. Prasad, Generalized elliptic restricted four-body problem with variable mass, *Astron. Lett.* 46 (2020), 275-288. <https://doi.org/10.1134/s1063773720040015>.
- [20] A.A. Ansari, K.R. Meena, S.N. Prasad, Perturbed six-body configuration with variable mass, *Romanian Astron. J.* 30 (2020), 135-152.
- [21] M.J. Zhang, C.Y. Zhao, Y.Q. Xiong, On the triangular libration points in photogravitational restricted three-body problem with variable mass, *Astrophys. Space Sci.* 337 (2011), 107-113. <https://doi.org/10.1007/s10509-011-0821-8>.
- [22] A.A. Ansari, Effect of albedo on the motion of the infinitesimal body in circular restricted three-body problem with variable masses, *Italian J. Pure Appl. Math.* 38 (2017), 581-600.
- [23] A.A. Ansari, The circular restricted four-body problem with triaxial primaries and variable infinitesimal mass, *Appl. Appl. Math.* 13 (2018), 818-838.
- [24] A.A. Ansari, R. Kellil, S.K. Sahdev, Dynamical behavior of an infinitesimal variable mass body in the elliptical hill problem, *Romanian Astron. J.* 32 (2022), 15-33.
- [25] E.I. Abouelmagd, A. Mostafa, Out of plane equilibrium points locations and the forbidden movement regions in the restricted three-body problem with variable mass, *Astrophys. Space Sci.* 357 (2015), 58. <https://doi.org/10.1007/s10509-015-2294-7>.
- [26] J.H. Jeans, *Astronomy and cosmogony*, Cambridge University Press, Cambridge, (1928).

- 
- [27] I.V. Meshcherskii, Works on the mechanics of bodies of variable mass, GITTL, Moscow, (1949).
- [28] L.G. Luk'yanov, On the restricted circular conservative three-body problem with variable masses, Astron. Lett. 35 (2009), 349-359. <https://doi.org/10.1134/s1063773709050107>.
- [29] F. Bouaziz, A.A. Ansari, Perturbed Hill's problem with variable mass, Astron. Nachr. 342 (2021), 666-674. <https://doi.org/10.1002/asna.202113870>.